

Sodium Channel Gating in Clonal Pituitary Cells

The Inactivation Step Is Not Voltage Dependent

GABRIEL COTA and CLAY M. ARMSTRONG

From the Department of Physiology, University of Pennsylvania, Philadelphia, Pennsylvania 19104-6085; and the Department of Physiology, Biophysics and Neurosciences, Centro de Investigacion y de Estudios Avanzados del Instituto Politecnico Nacional, AP 14-740, DF 07000, Mexico

ABSTRACT We have determined the time course of Na channel inactivation in clonal pituitary (GH₃) cells by comparing records before and after the enzymatic removal of inactivation. The cells were subjected to whole-cell patch clamp, with papain included in the internal medium. Inactivation was slowly removed over the course of 10 min, making it possible to obtain control records before the enzyme acted. Papain caused a large (4–100×) increase in current magnitude for small depolarizations (near –40 mV), and a much smaller increase for large ones (~1.5× at +40 mV). For technical reasons it was sometimes convenient to study outward I_{Na} recorded with no Na⁺ outside. The instantaneous I-V (IIV) curve in this condition was nonlinear before papain, and more nearly linear afterwards. The g_{Na}-V curve after papain, obtained by dividing the I_{Na}-V curve by the IIV curve, was left-shifted by at least 20 mV and steepened. A spontaneous 5–10 mV left shift occurred in the absence of papain. The rate of the inactivation step was found to vary only slightly from –100 mV to +60 mV, based on the following evidence. (a) Before papain, inactivation rate saturated with voltage and was constant from +20 to +60 mV. (b) We activated the channels with a brief pulse, and studied the time course of the current on changing the voltage to a second, usually more negative level (Na⁺ present internally and externally). The time course of inactivation at each voltage was obtained by comparing control traces with those after inactivation was removed. When the 5–10-mV spontaneous shift was taken into account, inactivation rate changed by <10% from –100 to +60 mV. The data are considered in terms of existing models of the Na channel.

INTRODUCTION

Na channels in excitable membranes open transiently in response to a depolarizing step and then inactivate, as first described by Hodgkin and Huxley (1952*a, b*) in the

Address reprint requests to Dr. Clay M. Armstrong, Department of Physiology, University of Pennsylvania, Philadelphia, PA 19104-6085.

squid giant axon. Their model assumes two parallel, voltage-dependent gating processes, activation and inactivation, which are completely independent of each other. After a depolarization, the several steps required for activation quickly open the channel, while inactivation is a relatively slow process that drives the channels into a nonconducting state that is distinct from the resting state.

Experimental support for the assumption that activation and inactivation are two separable processes was provided by the discovery that internal perfusion of a squid axon with pronase removes inactivation of I_{Na} without affecting the activation kinetics (Armstrong et al., 1973). However, the Hodgkin and Huxley model proved to be inadequate in explaining data from later experimental work, and it is now clear that activation and inactivation are not independent but "coupled" (see, e.g., Armstrong, 1981). Specifically, it has been postulated that all but the last of the several steps involved in activation must occur before the channel can inactivate.

The development of patch-clamp techniques (Hamill et al., 1981) has made possible the study of Na channel gating in mammalian cells, and single-channel experiments have been used to analyze inactivation in Na channels of neuroblastoma (Aldrich et al., 1983; Aldrich and Stevens, 1983, 1987) and clonal pituitary (GH₃) cells (Vandenberg and Horn, 1984). In most respects, the single-channel data have confirmed the mechanisms deduced from squid axon measurements (Bezanilla and Armstrong, 1977; Armstrong and Bezanilla, 1977; Armstrong and Gilly, 1979). The most important observations, which led to what will be called the squid model, were the following. (a) The Hodgkin and Huxley parameter τ_h does not measure one phenomenon (closing of the inactivation gate) but rather two: the occurrence of several, but not all, of the transitions that lead to opening of the activation gate (for convenience, this will be called "partial activation"), followed by closing of the inactivation gate. Partial activation is a prerequisite for closing of the inactivation gate. τ_h reflects the time required for partial activation, followed by the inactivation transition. (b) Channels can inactivate before they conduct (i.e., after partial activation), a prediction of the squid model that was first noted and confirmed by Bean (1981) with macroscopic measurements in crayfish axons, and confirmed by Aldrich and Stevens (1983) with single-channel measurements. (c) The opening of sodium channels continues until the pool of closed channels is exhausted, which takes surprisingly long for small depolarizations. The squid model predicted late openings (Bezanilla and Armstrong, 1977), and these were confirmed by single-channel measurements (Aldrich et al., 1983). (d) For large depolarizations, the time required for activation becomes negligible compared with inactivation, and current decay is limited only by the rate of the inactivation step. Thus current decay rate, or τ_h , is independent of voltage for large depolarizations, as observed by Aldrich and Stevens (1987) with single-channel measurements.

Conclusions from single-channel measurements on neuroblastoma cells, however, disagreed with those from GH₃ cells on several basic facts. Single Na channels in cell-attached membrane patches from neuroblastoma cells open at most one time during a depolarization and close directly into an inactivated state with a fast rate constant that is not dependent on membrane potential over most of the activation voltage range (Aldrich et al., 1983; Aldrich and Stevens, 1987). For GH₃ cells, on the other hand, a maximum-likelihood analysis of single Na channel currents in

excised (outside-out) membrane patches concluded that the inactivation step is inherently voltage dependent (Vandenberg and Horn, 1984). Further, for small depolarizations the activation gate of a given channel was likely to flicker open and closed numerous times before inactivation occurred. Neither of these differences obscured the basic adherence of the observations to the squid model.

A new aspect of the problem has been examined recently by Gono and Hille (1987). They found that papain and other proteolytic enzymes applied inside neuroblastoma cells remove inactivation of whole-cell Na currents. Concomitantly, they increase I_{Na} amplitude, greatly prolong the rising phase of I_{Na} for small depolarizations, and shift the peak g_{Na} -voltage curve in the negative direction by ~25 mV. Their conclusion is that these changes in macroscopic I_{Na} after the removal of inactivation are more readily explained by the gating models suggested by Bezanilla and Armstrong (1977) and Aldrich et al. (1983), in which inactivation follows nearly irreversible activation with a relatively high, voltage-independent rate constant.

Stimulated by Gono and Hille's article (1987) we have examined the effect of internally applied papain on the macroscopic activity of Na channels in GH₃ cells. We find that this treatment modifies the Na current of the pituitary cells in a similar way to that described for neuroblastoma cells. Most importantly, we have obtained direct experimental evidence that the inactivation step is not voltage dependent over a wide voltage range. A preliminary report of the results has appeared elsewhere (Armstrong and Cota, 1988).

METHODS

Cell Culture

GH₃ cells were obtained from the American Type Culture Collection (Rockville, MD), and maintained using standard culture methods, in Kennett's HY medium (Cell Center, University of Pennsylvania, Philadelphia, PA or Hazleton Research Products, Lenexa, KS) supplemented with 5% fetal bovine serum and 1% glutamine (Gibco Laboratories, Grand Island, NY). Once every 10 d the maintenance culture was split by using a brief trypsin digestion in a Ca- and Mg-free saline (trypsin-EDTA; Flow Laboratories, McLean, VA) to detach the cells, and by replating at sevenfold lower density. At the time of splitting, a fraction of the cells were replated on fragments of coverslips and placed in 35-mm plastic petri dishes. We used ~150 μ l of the cell suspension and 2 ml of fresh culture medium per dish. Experiments were carried out on these cells, usually 2 d after plating.

Experimental Chamber

The experimental chamber was 12 × 4 mm, and 2 mm deep, and was designed to make possible reasonably rapid changes of external solution (nearly complete exchange in ~30 s). Temperature was controlled within a fraction of a degree using a Peltier cooler, with a thermistor in the chamber as temperature sensor. The experiments were performed at 15–20°C, as indicated in the figure legends.

Solutions

The recording solutions and their composition are listed in Table I. The osmolarity of the external solutions was adjusted to ~300 mosmol, 7–10 mosmol hyperosmotic with respect to the internal solutions. We often included 0.2 mM CdCl₂ in the external medium in an

attempt to suppress current through Ca channels. With 1 or 2 mM Ca^{2+} in the external solution, I_{Ca} was generally small compared with I_{Na} even without Cd^{2+} , and disappeared rapidly when papain (see below) was applied internally, as evidenced by the disappearance of the slow component of ionic tail current. To remove inactivation of Na channels we introduced papain inside the cells (Gonoi and Hille, 1987). The enzyme (type IV, crystallized and lyophilized two times; Sigma Chemical Co., St. Louis, MO) was added to the internal solutions at a concentration of 1 mg/ml, and delivered into the cell through the patch pipette.

Whole-Cell Clamping and Data Acquisition

The macroscopic activity of Na channels in GH_3 cells was examined using whole-cell recording with patch pipettes (Hamill et al., 1981), with a 10-M Ω feedback resistor on the headstage amplifier (an OPA-111; Burr Brown Research Corp., Tucson, AZ). Cells selected for recording were almost spherical, 16–25 μm in diameter. Current responses were sampled at 10- or

TABLE I
Recording Solutions

External solutions	Na*	Ca	Choline	Cl	HEPES [†]
0 Na, 2 Ca	—	2	150	154	10
0 Na, 10 Ca	—	10	140	160	10
76 Na, 1 Ca	76	1	76	154	10
75 Na, 2 Ca	75	2	75	154	10
140 Na, 10 Ca	140	10	—	160	10

Internal solutions	Na	Cs	F	Cl	Glu [‡]	EGTA [‡]	HEPES [†]
130 Na, 20 F	130	—	20	20	90	10	10
130 Na, 100 F	130	—	100	30	—	10	10
39 Na, 20 F	39	—	20	20	90	10	10
39 Na, 100 F	39	91	100	30	—	10	10

*Concentrations are in millimolar.

[†]External pH adjusted to 7.30 with CsOH (Na-free solutions) or with NaOH.

[‡]Glutamate.

[†]EGTA and HEPES acids were neutralized (to pH 7.30) with CsOH.

20- μs intervals, and were stored and analyzed using an LSI-11/73 computer (Scientific Micro Systems, Inc., Mountain View, CA). Both patch-amplifier and interface for pulse generation, data sampling, and display were homemade. Linear components in the membrane current signals were subtracted out using the scaled current response to 50-mV hyperpolarizing pulses. Unless noted, the holding potential was -80 mV.

Patch Clamp and Supercharging

To improve clamp performance, we used "supercharging" (Armstrong and Chow, 1987); i.e., we added a voltage spike of appropriate size to the leading edge of the command step. The spike drives current rapidly through the electrode resistance, and is terminated precisely at the instant when membrane voltage (V_m) reaches the required level. Spike amplitude was adjusted by watching the current transient during the first 100 or 200 μs after the change in command voltage. For a square command, the transient has a very fast component corresponding to charging current for the stray capacitance of the electrode, and a slower component with a time constant approximately equal to the product of electrode resistance times

membrane capacitance. Spike amplitude is correctly adjusted when the slower component is nulled out.

To assure ourselves that V_m had the desired time course when supercharging was in use, we performed experiments with two patch electrodes on one cell. The clamp electrode was attached to the voltage clamp, which operated in the usual way to control V_m . The other electrode was attached to a follower that simply monitored performance. The output of the follower was not part of the feedback circuit. The follower electrode slightly increased the capacitance to be charged via the clamp electrode, but otherwise had no effect on performance. The slowly rising trace in Fig. 1 shows V_m , as measured by the follower, with a square command step. The trace is rounded, and rises with a time constant of $\sim 100 \mu\text{s}$. Measured empirically, the change is 79% complete after $170 \mu\text{s}$. After adjustment of the supercharging spike, the voltage change was much more rapid, and was 79% complete in $40 \mu\text{s}$ (rapidly rising trace in Fig. 1). The precise time course of the change was probably even faster, and

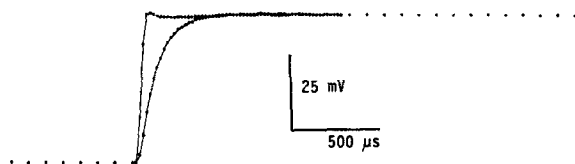


FIGURE 1. "Supercharging" speeds the change of membrane voltage. The two traces were recorded from a cell with two pipettes attached, one connected to a voltage (patch) clamp, the other to a follower. The patch clamp changed V_m by 50 mV, and the change was recorded by the follower. When supercharging was in use, V_m was within 3% of its final value in $60 \mu\text{s}$ (rapidly rising trace). Without supercharging, it took $400 \mu\text{s}$ to reach the same level of accuracy (slowly rising trace). Experiment Jn197G, cell no. 7., 20°C . Follower electrode resistance, $1.4 \text{ M}\Omega$. Clamp electrode resistance, $1.2 \text{ M}\Omega$. Borosilicate (BS) glass. 140 Na, 10 Ca//39 Na, 20 F.

has been filtered by the follower. Even so the figure shows that clamp performance is dramatically improved by supercharging.

Electrodes

Patch pipettes were fabricated from one of the following hard glasses: (a) borosilicate glass (KIMAX-51; Kimble Div., Owens-Illinois, Inc., Toledo, OH), and (b) aluminosilicate glass (Corning No. 1723; Gardner Glass, Claremont, CA or A-M Systems, Inc., Everett, WA). Pipettes were pulled in two steps. The coil of the puller usually was two turns of 1 mm nichrome wire (David Kopf Instruments, Tujunga, CA), shaped to 2.5 mm inside diameter and 2.3 mm length. Pipette tips were then carefully fire-polished to a bullet shape (this was easier

to do with aluminosilicate glass). Electrode resistance in most of the experiments was between 0.5 and 0.9 M Ω .

A Note on Terminology

"Inactivation" is used as in the Hodgkin and Huxley description to denote the decay of sodium current. This decay is measured by the empirical time constant τ_h , which is a function of membrane voltage (V_m). As noted in the Introduction, τ_h reflects the time course of both inactivation and the requisite preceding degree of activation. In this process, as we shall show, the inactivation step, from the "channel-open" state to the "inactivated" state, has a voltage-independent rate constant. Thus we will say that inactivation (in the Hodgkin and Huxley definition of the term) is voltage dependent, while the "inactivation step" is not.

Opening and closing of the channel activation gate will be referred to as "activation" and "deactivation." "Closing" of the channel can result from closing either the activation gate or the inactivation gate.

There is both fast (millisecond time range) and slow (seconds to minutes) inactivation of Na channels (e.g., Rudy, 1978). "Inactivation" here refers exclusively to fast inactivation.

Advantages of High Internal Na⁺

In many experiments we used a high Na⁺ concentration inside with no Na⁺ outside, and thus measured only outward current through the Na channels. This had two advantages. The first is that I_{Na} is easily visible at all voltages where the channels are activated. With normal Na⁺ concentrations I_{Na} is quite small near the Na⁺ equilibrium potential, i.e., above +30 mV. The second advantage is that the voltage error caused by the IR drop across the access resistance is less serious with outward than with inward current. As discussed by Gono and Hille (1987), access resistance errors are particularly worrisome on the downslope of the IV curve with high Na⁺ outside, since the error is in the direction to turn on additional Na channels, which in turn increases I_{Na} amplitude, produces a larger error, activates more channels, etc. This positive feedback cycle is averted when the current is outward. There is still an error, but it is smaller and its consequences are easy to understand.

RESULTS

Removal of Inactivation by Papain

The time course of papain action on outward I_{Na} at 0 mV is shown in Fig. 2 A. The time after break-in to the cell with the papain-containing patch pipette is given for each trace. The action of the enzyme was slow enough that control records could be obtained for several minutes after breaking into the cell, while inactivation was still intact. During the first minute or so there was often an increase in current magnitude by as much as 50%. This increase was also seen without papain in the pipette solution. After a minute or two, current magnitude usually stabilized, and the action of the enzyme became apparent over the next few minutes. In Fig. 2 A the first record shown is 2.2 min after break-in, and I_{Na} still inactivates fully. Removal of fast inactivation is practically complete ~7 min later. After 15 min the maximum current at this and other voltages slowly declined, with little further change in time course. Fig. 2 B presents another example of the change induced by intracellular papain on the macroscopic Na channel activity. In this case the Na⁺ equilibrium potential had a positive value, and current at 0 mV was inward.

In all the cells investigated ($n > 200$), peak I_{Na} increased with time for 6–12 min as the enzyme acted. The percentage increase depended on the membrane voltage, as pointed out by Goni and Hille (1987). Outward I_{Na} traces obtained at four voltages before and after papain action are shown in Fig. 3. At -10 mV the increase is very large, a factor of 10 in the experiment illustrated. The increase is progressively less dramatic at higher voltages (cf. Goni and Hille, 1987), a factor of 4.5 at 0 mV, 2.2 at $+20$ mV, and only 1.6 at $+40$ mV.

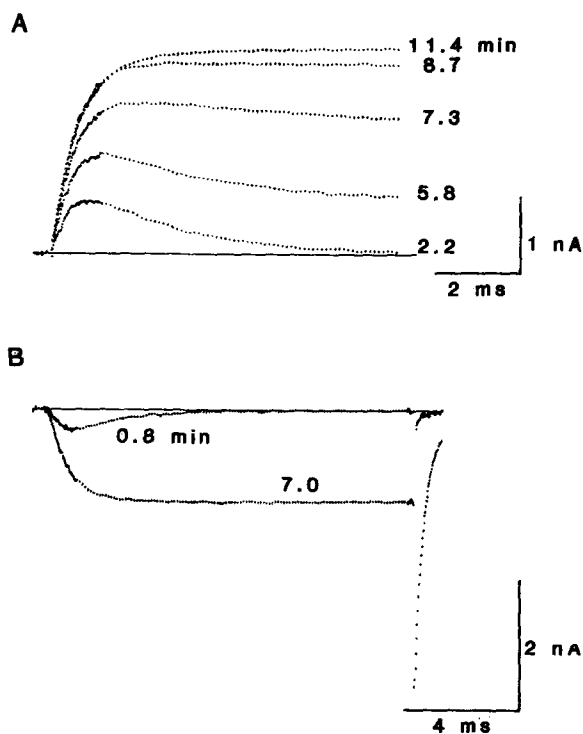


FIGURE 2. Removal of Na channel inactivation by intracellular papain. (A) A series of outward I_{Na} traces during voltage steps to 0 mV, obtained at different times (indicated by the numbers next to each trace) after breaking into a cell with a patch electrode containing papain. Na channels inactivate normally during the first 2–3 min. Complete removal of inactivation occurs within 10 min after break-in. (B) Papain action on inward I_{Na} . Na channel activity was induced by steps to 0 mV followed by repolarization to -80 mV. Traces were taken 0.8 min and 7.1 min after break-in. (A) Experiment J1307G, cell no. 6., 20°C . Electrode resistance (R_e) = 0.50 M Ω , aluminosilicate (AS) glass. 0 Na, 10 Ca, 0.2 Cd//130 Na, 20 F, papain. (B) Experiment Se107G, cell no. 5, 15°C . R_e = 0.60 M Ω , AS glass. 75 Na, 2 Ca, 0.2 Cd//39 Na, 100 F, papain.

Cell Capacitance

Under the influence of intracellular papain, cell shape often changed dramatically as papain destroyed the cell's internal architecture. A common early change was the evagination of large vesicles, rather like ears on a Mickey Mouse balloon. The final shape was usually a single transparent sphere, larger in diameter than the original cell, with a clump of intracellular material, presumably the remains of the cytoplasm, attached somewhere on the perimeter.

The changes in cell size and shape clearly raise the possibility that an increase in

membrane area is involved in the larger magnitude of I_{Na} after papain action. To test this point we measured membrane capacitance as the enzyme was acting, by applying a step of -50 mV and integrating the capacitive transient. In 15 cells, there was no significant change in the measured capacitance as the enzyme acted, although there was a large increase in I_{Na} , particularly for small depolarizations (see above). After prolonged papain treatment the capacitance sometimes declined noticeably. We conclude that an increase in membrane surface area does not play a part in the current magnitude increase.

Instantaneous Current-Voltage Curves

The instantaneous current-voltage (IIV) curve is a measure of the conducting properties of open channels as a function of voltage. The curve is measured by activating most of the channels with a strong, brief depolarization, stepping the membrane

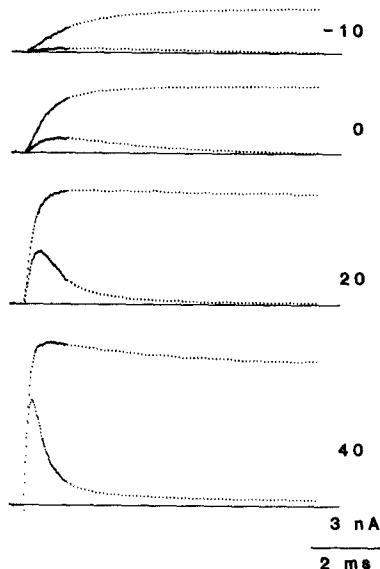


FIGURE 3. The change in I_{Na} after the removal of inactivation depends on voltage. The traces are Na currents induced by steps to various membrane potentials (indicated by the numbers at right) before (transient currents) and after papain action. The time after break-in was 1.5–1.8 and 7.0–7.3 min, respectively. Experiment J1307G, cell no. 2, 20°C, $R_c = 0.50$ M Ω , AS glass. 0 Na, 10 Ca, 0.2 Cd//130 Na, 20 F, papain.

potential to a new value, and measuring the current before, in theory, there is any change in the number of open channels.

The IIV curve changes shape after the action of papain, as shown in Fig. 4, where the before and after papain curves have been scaled to coincide at -10 mV. The control curve begins to flatten at about -10 mV, reaches a maximum value at $+20$ to $+30$ mV, and then declines to $\sim 90\%$ of its maximum at $+50$ mV. After papain, the curve is more nearly linear, continuing to rise until it saturates near $+50$ mV.

Open Channels as a Function of Voltage

In Figs. 2 and 3 it appears that papain increases the maximum number of open channels, most notably for small depolarizations. To quantitate this, it is necessary to take into account the change in the shape of the IIV curve. Specifically, the num-

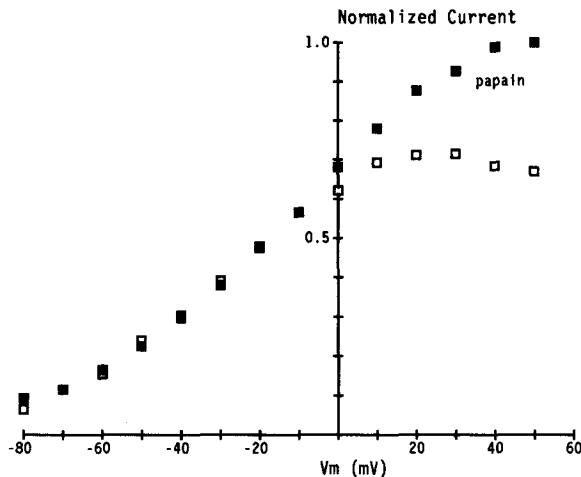


FIGURE 4. Papain removes a marked nonlinearity in the IIV curve, which is seen when there is no external Na. Na channels were activated by a 0.4-ms pulse to +60 mV, and V_m was then changed to the value given on the abscissa. Current was measured as soon as possible after the second step, usually ~ 30 or $40 \mu\text{s}$. The papain curve was normalized to the point at +50 mV. The control curve (*open squares*) was scaled to coincide with the papain curve at -10 mV. Experiment Au247H, cell no. 15, 15°C , $R_e = 0.6 \text{ M}\Omega$, AS glass. 0 Na, 2 Ca, 0.2 Cd//130 Na, 100 F, papain.

ber of open channels is proportional to the recorded current at a given voltage divided by the value of the IIV curve at that voltage. Curves plotting the fraction of open channels vs. voltage are given in Fig. 5. The curves are scaled to coincide at +40 mV. After papain, the open-channel curve is shifted to the left relative to the control. It is steeper, and reaches its saturation value far to the left of the control curve. We obtained results almost identical to those in Figs. 4 and 5 in two other cells.

It is necessary to consider the effect of access resistance errors on the shape of the open channel-voltage curve. With outward current the series resistance makes

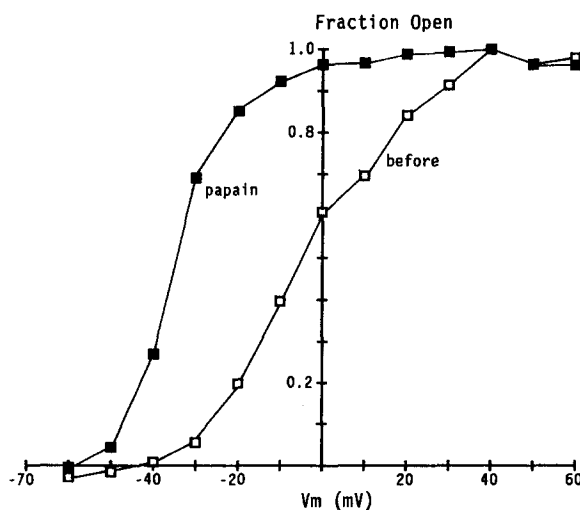


FIGURE 5. The curve relating the fraction of open channels to V_m is shifted to the left and steepened by papain. Maximum I_{Na} was measured from -60 to +60 mV, and the current at each voltage was divided by the IIV curve in Fig. 4 to yield the fraction of open channels. Same experiment as in Fig. 4.

the membrane voltage less positive than the applied value by an amount proportional to the amplitude of the current. Since current amplitude increases with voltage, the effect is to make the open channel-voltage curve somewhat less steep than it should be, particularly after papain when current magnitude is larger. Because electrode resistance in our experiments was low (0.5–0.9 M Ω) and current magnitude small (<5 nA) the access resistance error in most experiments probably did not exceed a few millivolts.

Rate of Decay of Macroscopic I_{Na}

As in many other cell-types, the time course of inactivation of macroscopic Na currents in GH₃ cells is voltage dependent (Dubinsky and Oxford, 1984; Matteson and

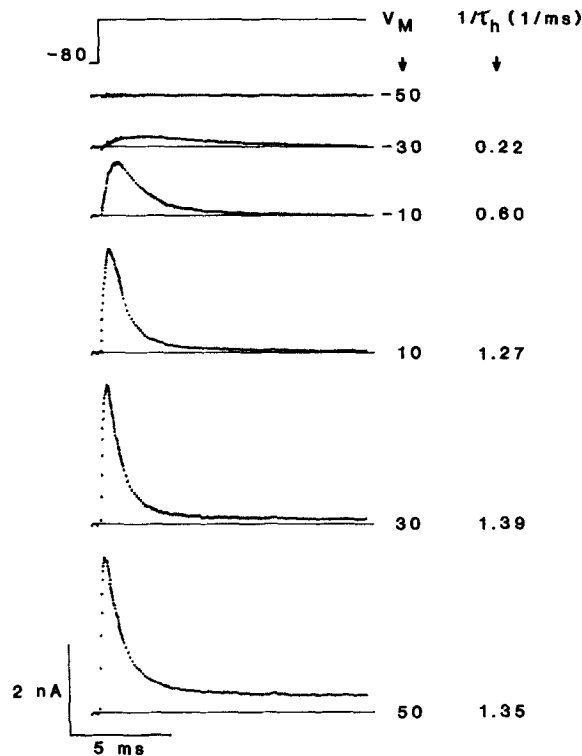


FIGURE 6. Family of outward Na currents at various membrane potentials (V_m , in mV). $1/\tau_h$ is the rate constant of a single exponential fit to the decaying phase of the outward I_{Na} . Experiment Au287G, cell no. 8, 15°C, $R_e = 0.90$ M Ω , BS glass. 0 Na, 2 Ca, 0.2 Cd//130 Na, 100 F.

Armstrong, 1984; Vandenberg and Horn, 1984). We have reexamined this voltage dependence for outward I_{Na} and the results are presented in Figs. 6 and 7. There was no papain in the pipette solution in these experiments. A family of outward I_{Na} traces obtained at various membrane potentials is shown in Fig. 6. Currents decay nearly to zero by the end of the 13-ms test pulse for voltages between -30 and 0 mV. Positive to 0 mV, currents decay to a steady-state level whose amplitude increases with depolarization. Current decay (after subtraction of the steady-state current) is well fit by a single exponential and the corresponding rate constant ($1/\tau_h$)

is indicated next to each trace. $1/\tau_h$ increases steeply with depolarization between -30 and $+10$ mV, but seems to saturate above $+20$ mV.

Saturation of $1/\tau_h$ at positive voltages is better illustrated in Fig. 7 A, in which it is shown that the decaying phase of the transient outward current recorded at $+20$ mV superimposes with that at $+30$ and $+50$ mV after appropriate scaling. This suggests that when channel activation is not rate limiting, as is probably the case for large depolarizations, inactivation of the Na channels develops with a rate constant that does not depend on voltage. Fig. 7 B plots the average value of $1/\tau_h$ obtained in seven different cells as a function of voltage. The saturating value of $1/\tau_h$ at positive voltages is close to 1.10 ms^{-1} on average. This value may correspond to the intrinsic

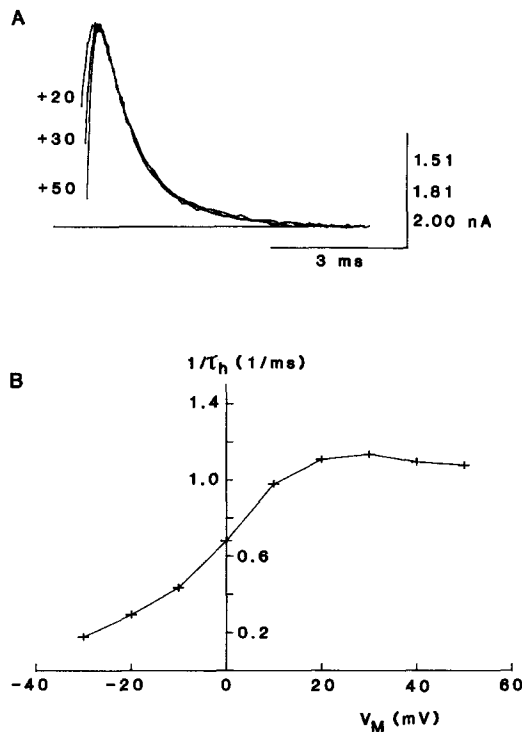


FIGURE 7. The rate for decay ($1/\tau_h$) of macroscopic I_{Na} saturates at positive voltages. (A) The transient outward current observed at $+50$ mV is compared with that recorded at $+20$ and $+30$ mV. The latter traces were scaled up by a factor of 1.32 and 1.10, respectively, and their position along the time axis was shifted to the left by different amounts so that current at 90% of the peak value coincides in the three cases. (B) Voltage dependence of $1/\tau_h$. $1/\tau_h$ increases e -fold per 24 mV for voltages between -30 and $+10$ mV, but has a practically constant value above $+20$ mV. (A) Experiment Au217H, cell no. 9, 15°C , $R_e = 0.9 \text{ M}\Omega$, BS glass. 0 Na, 2 Ca, 0.2 Cd//130 Na, 100 F. (B) Average values from seven cells. Solutions were the same as in A.

rate of inactivation of open Na channels. The voltage dependence of the inactivation step is explored below using a different experimental protocol.

Inactivation Rate for Open Channels

Open Na channels can close either by inactivating, or by deactivating (i.e., by closure of either the inactivation or the activation gate). We have determined the rate constant of the inactivation step by comparing I_{Na} traces at several voltages before and after the proteolytic removal of inactivation, as shown in Fig. 8, A and B. A brief activating pulse to $+60$ mV drives most of the Na channels into the open state. Voltage is then stepped to a new level to examine closing kinetics at various mem-

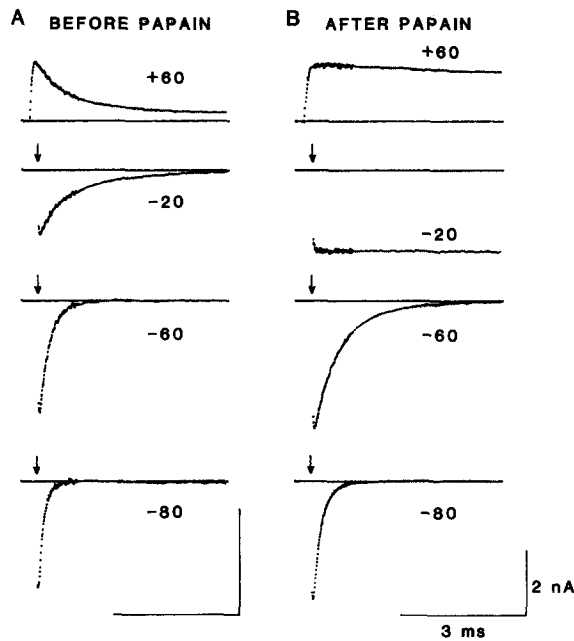


FIGURE 8. Na channel closing kinetics before (A) and after (B) removal of fast inactivation. Upper traces are outward I_{Na} recorded at +60 mV. Other traces are Na tails after repolarization to various voltage levels (indicated by the numbers next to each trace, in millivolts), after a 0.4-ms activating pulse to +60 mV. Arrows indicate the onset of repolarization. Records in A were obtained after 2.1–2.5 min of break-in, and those in B were obtained 6 min later. Same experiment as in Fig. 2B. Because electrode resistance was low (0.6 M Ω) we estimate that the series resistance error during the tails was acceptably small, probably 3 mV at maximum.

brane potentials. Records in Fig. 8A were obtained before action of intracellular papain. At every voltage channel closing is well fit by a single exponential. With inactivation intact, the rate constant of channel closing is the sum of the inactivation rate constant (k) and the deactivation rate constant (b). The contribution of b to the rate of closing can be studied separately by removing inactivation. Fig. 8B presents I_{Na} traces after the complete proteolytic removal of inactivation. Channels no longer close at or positive to -20 mV when the inactivation gate has been removed. This indicates that closing of unmodified channels at these voltages results from inactivation.

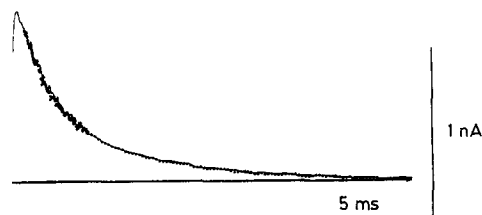


FIGURE 9. Open Na channels inactivate at +60 mV with the same rate that they inactivate at -20 mV. The transient outward current at +60 mV (continuous trace) and the inward Na tail at -20 mV (dotted trace) from Fig. 8A are plotted to compare the time course of inactivation at two different voltages. The Na tail is plotted upside down and has been scaled 0.75 \times to match the amplitude of the outward Na current at +60 mV at the time of the tail peak. No significant effect of voltage on the time course of I_{Na} inactivation is observed.

The time course of inactivation at -20 mV is compared with that at $+60$ mV in Fig. 9. Here the inward Na tail at -20 mV (from Fig. 8 A) has been plotted upside down and scaled so that the peak of the tail matches the value of the transient outward current at $+60$ mV. Superposition of these two traces is nearly perfect, indicating almost no change in the rate of channel closing despite the 80-mV difference in voltage. The same result was obtained in all of the six cells tested. Thus, the rate of inactivation is not dependent on voltage from -20 to $+60$ mV.

At more negative voltages, the deactivation rate b must be determined before cal-

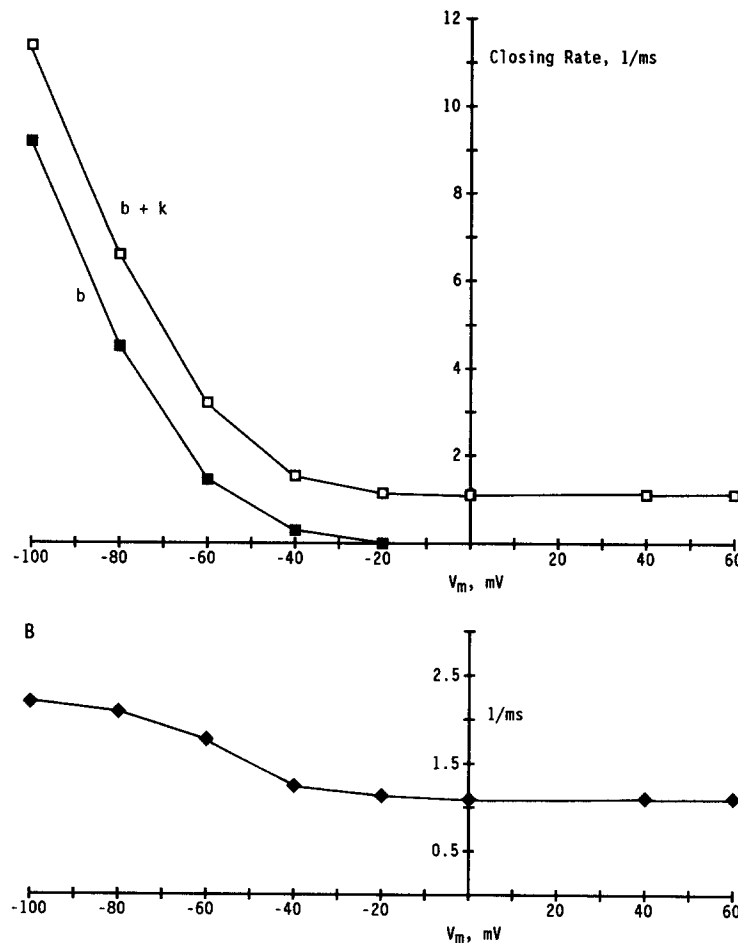


FIGURE 10. Voltage dependence of the closing rate for Na channels. (A) The closing rates for normal (inactivation intact; *open squares*) and modified (inactivation removed; *filled squares*) channels are plotted as a function of voltage. Closing rate values were obtained from I_{Na} traces recorded using the same experimental protocol as in Fig. 8. Records were taken 2.6–3.6 and 8.1–9.1 min after break-in. (B) The difference between the two curves in A is plotted vs. V_m . This curve shows a small voltage dependence that is probably artifactual (see text). Experiment Se107G, cell no. 2, 15°C , $R_c = 0.55 \text{ M}\Omega$, AS glass. 75 Na, 2 Ca, 0.2 Cd//39 Na, 100 F, papain.

culating k . We estimated b from the rate of closing in the absence of inactivation, by the following method. (a) Negative to -40 mV, the opening rate is negligible (as is evident from the absence of steady-state current), and the rate constant of the tail after papain gives b directly. (b) At -40 mV, where both a and b are finite, determination of b is slightly more complex. As an approximation, we used a two-state model (closed and open) with opening and closing rate constants a and b . For this model, steady-state current is $a/(a + b)$, and the rate constant is $a + b$. Thus b can be approximated, from the steady-state current and the rate constant. This approximation, which was necessary only for the point at -40 mV, seems to give a reasonable value, as judged from the smoothness of the curve.

b is plotted as a function of voltage in Fig. 10 A (filled squares). The open squares are the closing rate ($b + k$) for channels before papain action. The difference between the two curves in Fig. 10 A is the inactivation rate of open channels, k . This

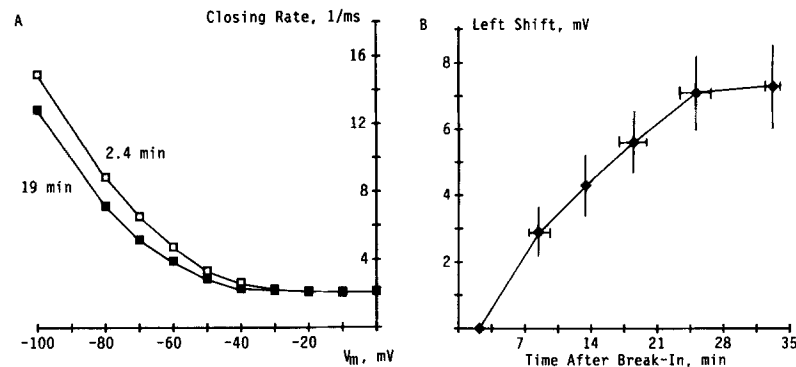


FIGURE 11. Spontaneous change in Na channel closing kinetics. (A) Voltage dependence of the closing rate 2.4 and 19 min after break-in. Each run was completed within 1 min. The same curve drawn through the 2.4-min points fits the 19-min points after shifting -7 mV along the voltage axis. (B) Left shift of the closing rate vs. voltage curve as a function of time under whole-cell recording. The points are the average for four cells, and the vertical bars give the standard errors. The horizontal bars give the range for the time of the measurements, which were not exactly the same in all four cells. Experiments Au287G, cells 5 and 7; Se027G, cells 2 and 5, 15°C , $R_c = 0.55 \text{ M}\Omega$, AS glass. 76 Na , $1 \text{ Ca}/39 \text{ Na}$, 100 F .

difference is plotted as a function of voltage in Fig. 10 B. Apparently k has a strange voltage dependence: it changes negligibly between -40 and $+60$ mV, but seems to increase somewhat from -40 to -100 mV. Even this small voltage dependence (e -fold/99 mV) of k is probably artifactual, and can be explained by a "spontaneous" change in Na channel kinetics, not related to papain action.

The spontaneous change in closing kinetics of Na channels in a cell internally dialyzed with a papain-free solution is illustrated in Fig. 11. The rate of closing determined within 2.4–3.4 min after breaking into the cell with the patch pipette (open squares) and 16.6 min later (filled squares) is plotted as a function of voltage in Fig. 11 A. Prolonged dialysis slows closing kinetics for voltages negative to -30

mV, whereas positive to this voltage the rate of closing is unaffected. The curve through early points was drawn by eye, and after shifting about -7 mV the same curve adequately fits the late points. Thus, effects of prolonged dialysis on Na channel closing kinetics can be expressed as a shift of the deactivation rate-voltage (k vs. V_m) relationship toward negative potentials, with no change in the rate of inactivation. The left shift in closing kinetics is dependent on time, as shown in Fig. 11 *B*. The shift was determined in four cells without papain, and the curve gives the average result and the standard error. We also observed left shifts in the g - V_m curve and in the curve relating $1/\tau_h$ to voltage. Similar shifts have been observed in previous studies of Na channels using whole-cell recording with patch pipettes in GH₃ cells (Fernandez et al., 1984; Goni and Hille, 1987) and other preparations (Marty and Neher, 1983; Goni et al., 1985; Fozzard et al., 1986).

If it is assumed that a similar "spontaneous" shift of the k - V_m relation occurs during (but unrelated to) papain treatment, the closing rate values in Fig. 10 *A* can be

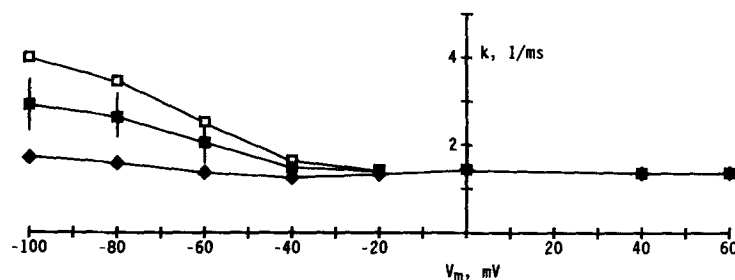


FIGURE 12. The average k - V curve for four cells is shown, with and without correction for the shift illustrated in Fig. 11. The open squares are uncorrected. The filled squares are the same data, but corrected for the shift that would occur in a control cell (no papain) after the same time of perfusion. The diamonds are the same data corrected for the maximum shift seen in Fig. 11 *B*. The vertical bars give the standard error, which was about the same for all three curves. At and positive to -40 mV the standard error is smaller than the symbols. Experiments Au 217G, cells 3 and 5; Se107G, cells 2 and 5, 15°C , $R_c = 0.55$ or 0.60 M Ω , AS glass. Solutions were the same as in Fig. 10.

corrected for the shift. Fig. 12 is a plot of k as a function of voltage, averaged from four cells, with and without correction for the shift. The open squares are the average curve for the four cells without correction. The filled squares are corrected assuming that the shift in the papain-treated cells develops at the same rate as in the absence of papain. Finally, on the chance that the shift may occur more rapidly with papain, the diamonds are the average curve corrected for the maximum shift seen in Fig. 11 *B*.

For all three curves, voltage dependence is negligible from -40 to $+60$ mV. Between -40 and -100 mV the voltage dependence is small in the uncorrected case (e -fold/68 mV) and very small or negligible in the corrected cases. We conclude that the rate constant for the transition of open Na channels into the inactivated state has no significant voltage dependence over the range -100 to $+60$ mV.

A Summary of the Properties of the Inactivation Rate

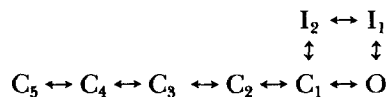
Results in the previous section indicate that the rate constant of the inactivation step (k) is voltage independent and that under our experimental conditions is unaffected by prolonged dialysis. In other experiments we have observed that k is not modified by raising the external Ca^{2+} concentration from 2 to 10 mM, although activation kinetics are greatly altered by this Ca change. k varies considerably from one cell to another, ranging from 0.8 to 2.2 ms^{-1} (15°C).

DISCUSSION

Proteolytic agents have proved very useful in analyzing the mechanism of Na channel inactivation, but there remain numerous points of uncertainty regarding both inactivation and the action of these agents. This discussion is organized around these uncertain points. The literature is reviewed in each case, and we present what we think to be the most plausible conclusions.

Voltage Dependence of the Inactivation Step

As reviewed in the Introduction, it is now accepted that much of the apparent voltage dependence of inactivation derives from coupling between the activation and inactivation gates. A quantitative model along these lines (Armstrong and Gilly, 1979) postulated that inactivation could occur from the fully activated state, or from the closed state that immediately preceded the conducting state:



(Scheme 1)

The inactivation steps ($\text{C}_1 \rightarrow \text{I}$, $\text{O} \rightarrow \text{I}$) in this model had negligible voltage dependence, corresponding to the movement of 0.15 electronic charges across the membrane. Bean (1981) noted that his macroscopic current measurements in crayfish axons were in reasonable agreement with this model. Subsequent studies with single channels (Aldrich et al., 1983; Aldrich and Stevens, 1983; Horn and Vandenberg, 1984) were interpreted in terms of similar models, but somewhat simplified, since gating current measurements giving detailed information regarding the closed states was not available in neuroblastoma or GH_3 cells.

Special attention has been given to the voltage dependence of the open to inactivated transition, $\text{O} \rightarrow \text{I}$. Aldrich et al. (1983) and Aldrich and Stevens (1987) concluded that this inactivation step in neuroblastoma channels has very little (if any) voltage dependence with an equivalent gating charge of <0.5 electronic charges (e -fold/50 mV). In GH_3 cells, however, Vandenberg and Horn (1984) concluded that open channels inactivate with a rate constant (β_1 in their terminology) that is voltage dependent. As discussed clearly by Horn and Vandenberg (1986), the degree of voltage dependence of the inactivation step is model dependent. It seems generally agreed that the lifetime of open Na channels is not very voltage dependent (e.g., Fig. 6 A of Horn and Vandenberg, 1984). In their analysis, then, voltage depen-

dence of β_1 is invoked not to explain a change in lifetime, but to explain the voltage dependence of P_1 , the probability that an open channel inactivates (see their paper for a precise definition of P_1). Horn and Vandenberg (1986) point out the difficulties in estimating P_1 , and these difficulties seem to underly the marked variability in the voltage dependence of β_1 that is seen in their experiments (e -fold/38 mV to e -fold/8 mV). It may be significant that the voltage dependence was low (e -fold/42 mV) in the relatively direct experiments in which inactivation was removed proteolytically (Fig. 10 of Horn et al., 1984).

Our results show unequivocally that the inactivation step is voltage independent from +60 to -40 mV, and probably from +60 to -100 mV as well. This extends well into the range (-50 to -20 mV) where Vandenberg and Horn (1984) detected voltage sensitivity of the inactivation rate constant. Negative to -40 mV some uncertainty is introduced in our determinations by a small left shift of the curves relating conductance and closing rate to voltage, a shift that is not related to papain (Fig. 11). Such shifts have also been observed by others (Fernandez et al., 1984; Gonoï and Hille, 1987). If no correction is applied for this shift, the inactivation rate changes by a factor of 2 between -40 and -100 mV, decreasing with depolarization. The change occurs in the voltage range where the contribution of the activation gate to current decay rate is very sensitive to voltage; i.e., between -50 and -20 mV. Although it cannot be proved definitively, the strong inference is that the change in decay rate results from shifts in the properties of the activation gate, like the ones in Fig. 11, and that the inactivation rate is not voltage sensitive. With or without correction there is no voltage dependence positive to -40 mV, and in the uncorrected case, a small voltage dependence negative to -40 mV.

How Many Times Does a Channel Open and Close before Inactivating?

An open Na channel can cease to conduct either because its activation gate closes (deactivation), or because its inactivation gate closes. The relative probabilities of the two fates of an open channel have been a subject of dispute, with Vandenberg and Horn (1984) maintaining that in pituitary cells at potentials more negative than -10 mV, the activation gate closes and opens several times before inactivation occurs, while Aldrich and Stevens (1987) say that neuroblastoma Na channels open only once and then inactivate.

In the present work, information on this question is contained in the curves showing the rate constants b (for deactivation) and k (for the inactivation step) as a function of voltage (Figs. 10 and 12). The b and k curves cross at about -55 mV in Fig. 12. Negative to this voltage, where b is larger than k , the activation gate is most likely to close, and positive to -55 mV the reverse is true. At -40 mV, the channel has about one chance in five of deactivating, and about four chances in five of inactivating. Positive to -20 mV it is almost a certainty that the channel will inactivate.

These numbers are in good qualitative agreement with the effects on channel lifetime reported by Patlak and Horn (1982), working on Na channels in excised patches from rat myotubes. They found that removal of inactivation with *N*-bromoacetamide prolonged channel lifetime at -40 mV by a factor of 10-fold. Our curve would predict a 10-fold prolongation at -30 mV. In squid axons, where inactiva-

tion is relatively slow, the probability of deactivation rather than inactivation must be much higher.

Why Does Papain Increase Current, Particularly for Small Depolarizations?

Gonoi and Hille (1987) explained the large increase in current at small depolarizations with the following kinetic diagram:

closed \rightarrow open \rightarrow inactivated

(Scheme 2)

They pointed out that at low voltage, the opening transitions are slow compared with the inactivation step. Consequently, the concentration of channels in the open state is never very high: the channels trickle into the open state and inactivate quickly. In this situation, removing inactivation greatly increases the maximum concentration in the open state, by eliminating the main exit path from this state. Gonoi and Hille assumed that above -40 mV the closed to open transition was effectively irreversible, so that after papain, all channels would eventually be in the open state above this voltage. At very high voltage, the opening transitions are much faster than the inactivation step, and the effect of removing inactivation is much less marked.

We generally agree with these considerations, but we find that after papain, the opening transition is effectively irreversible only above -20 mV. Also, there may be another factor underlying the current increase seen for small depolarizations as papain acts. As discussed in the Introduction, it is possible for Na channels to inactivate before they conduct, by following the path from closed state C_1 directly to inactivated state I_2 (see scheme 1). Clearly removing this pathway would increase the current magnitude. This could be investigated and quantitatively modeled, but our data have two uncertainties, the spontaneous left shift of activation gating, and the change in shape of the instantaneous current voltage curve after papain, that are too large to make this worthwhile at present.

Left Shift of the g-V Curve after Papain

In addition to the small "spontaneous" shift noted in Fig. 11, there is after papain a larger left shift and a pronounced steepening of the $g-V_m$ curve. These effects can be explained by the same factors that increase the size of the current for small depolarizations. Such a shift was not seen in squid axons acted on by pronase (Armstrong et al., 1973; Stimers et al., 1985) or *N*-bromoacetamide. (Oxford et al., 1978). A probable reason for the difference between papain on GH_3 cells and pronase on squid axons is that the inactivation step is very slow relative to activation in squid axons.

Original version received 21 September 1988 and accepted version received 9 March 1989.

REFERENCES

- Aldrich, R. W., D. P. Corey, and C. F. Stevens. 1983. A reinterpretation of mammalian sodium channel gating based on single channel recording. *Nature*. 306:436-441.

- Aldrich, R. W., and C. F. Stevens. 1983. Inactivation of open and closed sodium channels determined separately. *Cold Spring Harbor Symposia on Quantitative Biology*. 48:147–153.
- Aldrich, R. W., and C. F. Stevens. 1987. Voltage-dependent gating of single sodium channels from mammalian neuroblastoma cells. *Journal of Neuroscience*. 7:418–431.
- Armstrong, C. M. 1981. Sodium channels and gating currents. *Physiological Reviews*. 61:644–683.
- Armstrong, C. M., and F. Bezanilla. 1977. Inactivation of the sodium channel. II. Gating current experiments. *Journal of General Physiology*. 70:567–590.
- Armstrong, C. M., F. Bezanilla, and E. Rojas. 1973. Destruction of sodium conductance inactivation in squid axons perfused with pronase. *Journal of General Physiology*. 62:375–391.
- Armstrong, C. M., and R. H. Chow. 1987. Supercharging: a method for improving patch-clamp performance. *Biophysical Journal*. 52:133–136.
- Armstrong, C. M., and G. Cota. 1988. Open sodium channels inactivate with a voltage-independent rate constant in pituitary cells. *Biophysical Journal*. 53:14a. (Abstr.)
- Armstrong, C. M., and W. F. Gilly. 1979. Fast and slow steps in the activation of sodium channels. *Journal of General Physiology*. 74:691–711.
- Bean, B. P. 1981. Sodium channel inactivation in the crayfish giant axon. Must a channel open before inactivating? *Biophysical Journal*. 35:595–614.
- Bezanilla, F., and C. M. Armstrong. 1977. Inactivation of the sodium channel. I. Sodium current experiments. *Journal of General Physiology*. 70:549–566.
- Dubinsky, J. M., and G. S. Oxford. 1984. Ionic currents in two strains of rat anterior pituitary tumor cells. *Journal of General Physiology*. 83:309–339.
- Fernandez, J. M., A. P. Fox, and S. Krasne. 1984. Membrane patches and whole-cell membranes: a comparison of electrical properties in rat clonal pituitary (GH₃) cells. *Journal of Physiology*. 356:565–585.
- Fozzard, H. A., D. A. Hanck, J. C. Makielski, and M. F. Sheets. 1986. Shift in inactivation and activation parameters of Na⁺ current in internally dialyzed canine cardiac Purkinje cells. *Journal of Physiology*. 371:194P. (Abstr.)
- Gonoi, T., and B. Hille. 1987. Gating of Na channels. Inactivation modifiers discriminate among models. *Journal of General Physiology*. 89:253–274.
- Gonoi, T., S. J. Sherman, and W. A. Catterall. 1985. Voltage clamp analysis of tetrodotoxin-sensitive and -insensitive sodium channel in rat muscle cells developing *in vitro*. *Journal of Neuroscience*. 5:2559–2564.
- Hamill, O. P., A. Marty, E. Neher, B. Sakmann, and F. J. Sigworth. 1981. Improved patch-clamp techniques for high-resolution current recording from cells and cell-free membrane patches. *Pflügers Archiv*. 391:85–100.
- Hodgkin, A. L., and A. F. Huxley. 1952a. The dual effect of membrane potential on sodium conductance in the giant axon of *Loligo*. *Journal of Physiology*. 116:497–506.
- Hodgkin, A. L., and A. F. Huxley. 1952b. A quantitative description of membrane current and its application to conduction and excitation in nerve. *Journal of Physiology*. 117:500–544.
- Horn, R., and C. A. Vandenberg. 1984. Statistical properties of single sodium channels. *Journal of General Physiology*. 84:505–534.
- Horn, R. and C. A. Vandenberg. 1986. Inactivation of single sodium channels. *In Ion Channels in Neural Membranes*. Alan R. Liss, New York. 71–83.
- Horn, R., C. A. Vandenberg, and K. Lange. 1984. Statistical analysis of single sodium channels. Effects of *N*-bromoacetamide. *Biophysical Journal*. 45:323–335.
- Marty, A., and E. Neher. 1983. Tight-seal whole-cell recording. *In Single-Channel Recording*. B. Sakmann and E. Neher, editors. Plenum Press, New York. 107–122.

- Matteson, D. R., and C. M. Armstrong. 1984. Na and Ca channels in a transformed line of anterior pituitary cells. *Journal of General Physiology*. 83:371–394.
- Oxford, G. S., C. H. Wu, and T. Narahashi. 1978. Removal of sodium channel inactivation in squid axons by *N*-bromoacetamide. *Journal of General Physiology*. 71:227–247.
- Patlak, J., and R. Horn. 1982. Effect of *N*-bromoacetamide on single sodium channel currents in excised membrane patches. *Journal of General Physiology*. 79:333–351.
- Rudy, B. 1978. Slow inactivation of the sodium conductance in squid giant axons. Pronase resistance. *Journal of Physiology*. 283:1–21.
- Stimers, J. R., F. Bezanilla, and R. E. Taylor. 1985. Sodium channel activation in the squid giant axon. Steady state properties. *Journal of General Physiology*. 85:65–82.
- Vandenberg, C. A., and R. Horn. 1984. Inactivation viewed through single sodium channels. *Journal of General Physiology*. 84:535–564.